ACS Sustainable Chemistry & Engineering

Research Article

Cite This: ACS Sustainable Chem. Eng. XXXX, XXX, XXX−XXX

High-Performance Strain Sensors Based on Spirally Structured Composites with Carbon Black, Chitin Nanocrystals, and Natural Rubber

Yongwang Liu, Fan Wu, Xiujuan Zhao, and Mingxian Liu*

Department of Materials Science and Engineering, Jinan University, Guangzhou 510632, P.R. China

Supporting Information

ABSTRACT: In this research, a new type of conductive composite with high tensile strength, high elasticity, and cost competitiveness has been developed through solution mixing−spraying−rolling methods. Naturel rubber (NR) latex with chitin nanocrystals (ChNCs) as reinforcing filler and carbon black (CB) are thermally sprayed on glass substrate layer by layer, and then, spirally structured conductive composites are obtained by rolling the sheets. When the CB content is 4.44%, the conductivity of the NR/ChNCs-CB composite can reach 6.92 s/m. The tensile strength of 5% ChNCs reinforced conductive composites is 3.47 MPa, which is 3.1 times that of NR-CB composites without ChNCs. The strain sensor exhibits a high gauge factor (GF ≈ 5) and electrical conductivity stability in a small deformation range and still shows good stability and recoverability upon 25%, 50%, and 100% strain. The high-sensitivity strain sensors are further employed for monitoring human activities such as finger movements and pronunciation, which shows good reproducibility and reliability. This study provides a routine of preparing highly stretchable and multifunctional strain sensors based on inexpensive raw materials by a simple manner, which opens up new opportunities for the development of stretchable electronic devices.

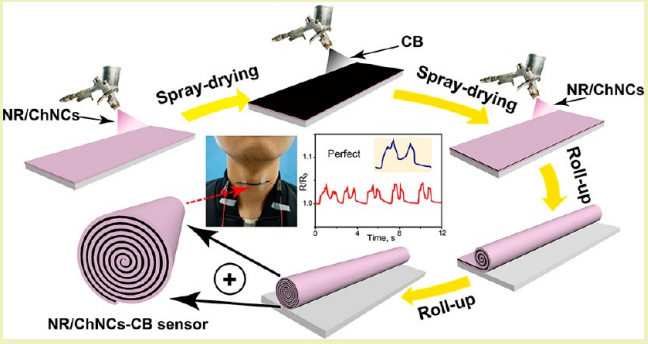

KEYWORDS: *Spiral structure, Chitin nanocrystals, Strain sensor, Thermal spray, Carbon black*

INTRODUCTION

To meet the requirements of wearable devices, flexible and stretchable electronics have been developed, such as electrodes, transistors, sensors, generators, batteries, supercapacitors, antenna, etc.[1−9] With the development of scalable and sensitive sensors, conductors with rapid response and high conductivity have become a focal point for many new applications, such as personal machine interfaces, motion sensors, retractable displays, wearable electronics, and artificial muscles.[10−18] Traditional resistive sensors are commonly used in wearable devices because of their high sensitivity to external forces.[19−21] However, traditional strain sensors have significant drawbacks for practical applications because they can only withstand very limited stresses before breaking (<5%).[5,22] Therefore, new types of sensors should be prepared by the materials which have both good electrical conductivity and high stretchability.[10,23−26]

The core of stretchable equipment is a flexible conductive material, and the material structure can be variously designed. For example, network structures,[27] porous structures,[28,29] wave structures,[30,31] spiral structures,[32−34] and cross-stacked structures[23] have been developed for this purpose in recent years. For different material structures, the conductive materials of the retractable electronic device are usually deposited on the surfaces of the substrate. When the repeated deformation occurs, the conductive materials will fall off from the substrates easily, resulting in the failure of the sensor device. Recently, Lee et al.[35] found that highly stretchable metal electrodes can be obtained by solution treatment of very long metal nanowires (>100 μm) and subsequent infiltration networks formed by low-temperature nanowelding, which will overcome the performance limitation of stretchable electronic devices (such as graphene,[36,37] carbon nanotubes,[38,39] and curved nanobelt[40]). Muth et al.[41] found that the new method of embedded 3D printing enables the fabrication of strain sensors in highly conformal and stretchable elastomeric matrices. Despite such groundbreaking achievements, these systems involve complex chemical synthesis and process processes. Therefore, it is still a great challenge to develop a simple, scalable, economically efficient, and environmentally friendly manufacturing technology to produce extensible electronic products using commercial materials.

In this study, a new type of conductive composite with high tensile strength, high elasticity, and cost competitiveness has

Received: April 28, 2018
Revised: May 23, 2018
Published: June 11, 2018

DOI: 10.1021/acssuschemeng.8b01933
ACS Sustainable Chem. Eng. XXXX, XXX, XXX−XXX

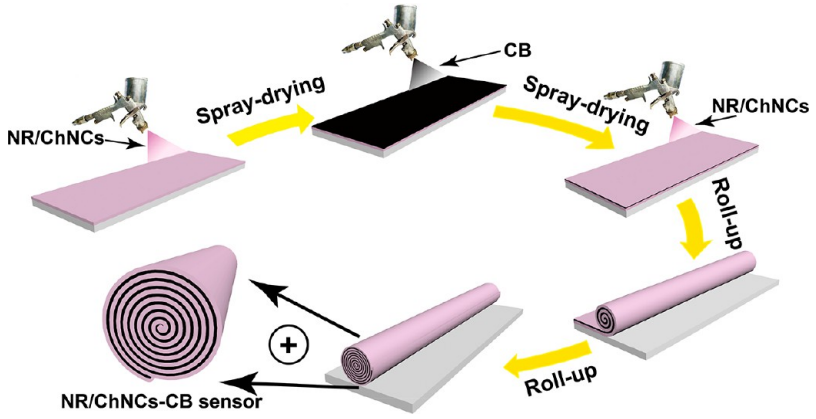

Figure 1. Schematic diagram for preparation of spirally layered NR/ChNCs-CB composites.

been prepared by solution mixing and a subsequent spraying–drying method. A spirally structured conductive composite of natural rubber (NR)/chitin nanocrystals (ChNCs)-carbon black (CB) is obtained by rolling the sheets. There are two main advantages of spirally layered structures for strain sensor application. On the one hand, a spirally layered structure can protect the conductive layers from abrasion under diverse harsh conditions, endowing the composites with satisfactory conductive stability during application.[10] On the other hand, a spirally layered structure can obtain high conductivity with a small amount of conductive filler without a harsh long dispersion process. The disadvantage of spirally layered structures is that the matrix material must have high adhension ability toward the conductive layer and should have flexibility ensuring that the composites can be rolled up. NR has good adhesion and can be used as a good elastic material, but the tensile strength and resilience of pure NR are poor. So NR needs to be reinforced by the addition of nanofillers. As an one-dimensional nanomaterial, ChNCs have a high aspect ratio, high strength, low density, and renewable characteristics.[42,43] The tensile strength of ChNCs is 7.5 GPa, and the transverse modulus and longitudinal modulus are 150 and 15 GPa, respectively, which show a high reinforcing effect for different polymers.[44] Based on the author's previous research on NR/ChNCs,[45] 5 wt % ChNCs were used to enhance NR in this work. A CB ethanol suspension is then sprayed on the NR/ChNCs composite film. Because there is no strong interfacial interactions between CB and rubber, the conductive layer is easily destroyed. It is necessary to add another layer of NR/ChNCs composite film on the surface of the CB layer and get a sandwich-structured composite. Then, the three-layer film is rolled into strips. NR/ChNCs film is tightly bonded together with the CB layer to form a stable NR/ChNCs-CB conductive composite with a spirally layered structure. The composites have the characteristics of good conductivity, good stretchability, a stable structure, and variable strain sensitivity. These advantages allow the composite to be prepared as a multifunctional sensor for monitoring small and large human activities and as a sensor fiber for wearable electronic products. The research can be used to prepare highly extensible and multifunctional electronic products on the basis of such cheap raw materials in a simple way, which opens up a wide range of new opportunities for the manufacture and application of extensible electronic devices.

EXPERIMENTAL SECTION

Materials. Natural rubber (without curing agent, solid content 60%) was purchased from Dongguan Tunchang Xinyuan Rubber Trade Co., Ltd. Conductive carbon black (BP2000) was bought from Shanghai Cabot Chemical Co., Ltd. Chitin and hydrochloric acid were provided by Shanghai Aladdin Bio-Chemical Technology Co., Ltd. Ethanol was obtained from Tianjin Fine Chemicals Co., Ltd. The ultrapure water used in the experiment was filtered by Millipore purification equipment. All chemicals are analytical grade and can be used without any purification.

Preparation of NR/ChNCs and CB Ethanol Dispersions. ChNCs were prepared via acid hydrolysis according to the previous report.[46] First, 0.3 g of ChNCs was added to 50 mL water and then sonicated at a power of 570 W for 1 h to obtain a uniform ChNCs dispersion. Meanwhile, 10 g of NR latex (solid content of latex was 60%) was diluted to 50 mL with water. After that, the ChNCs dispersions were added to dilute NR latex under stirring conditions for 5 h, and uniform 5% NR/ChNCs dispersions were obtained. CB ethanol dispersion was prepared by adding 0.2 g of CB to 100 mL of ethanol followed by sonication for 20 min at 570 W power.

Preparation of Spirally Layered Structure NR/ChNCs-CB Conductive Composites. The preparation process of the NR/ChNCs-CB composite with a spirally layered structure is shown in Figure 1. First, a commercial spray gun was used to evenly spray the prepared NR/ChNCs dispersion on a glass slide. Because the slide is in the condition of constant temperature heating at 60 °C, the rubber mixture will quickly form a thin layer of rubber film on the slide. Afterward, a CB layer was sprayed on the rubber layer by spraying the CB ethanol dispersion at the concentration of 2 mg/mL. When the concentration was larger than 2 mg/mL, it was easy to result in clogging of the spray gun and inhomogeneous coating. When the concentration was lower than 2 mg/mL, the preparation process was time consuming due to the low concentration especially for the sample with high CB content. Because there was no interaction force between CB, the CB layer needed to be covered with another layer of rubber film by thermal spraying of the NR/ChNCs dispersion. Finally, the sandwich-structured NR/ChNCs-CB composite was stripped from the glass sheet by rolling it up, and the spirally layered structure of the NR/ChNCs-CB composite was obtained. The NR-CB composite was also prepared with a similar procedure but without the addition of ChNCs.

Preparation of NR/ChNCs/CB Composites. The ternary NR/ChNCs/CB composites were prepared by a solution mixing–casting method. While preparing the NR/ChNCs dispersion, a certain amount of CB was dispersed in ammonia–water and uniformly dispersed under ultrasonic treatment, and CB/ammonia–water was mixed with NR/ChNCs dispersion via mechanical stirring. The dispersion was then poured into a square PTFE dish and dried in a 60 °C oven.

Characterizations. *Stereo Microscope.* The cross sections of the NR/ChNCs-CB composite and the CB layer without covering of the

DOI: 10.1021/acssuschemeng.8b01933
ACS Sustainable Chem. Eng. XXXX, XXX, XXX–XXX

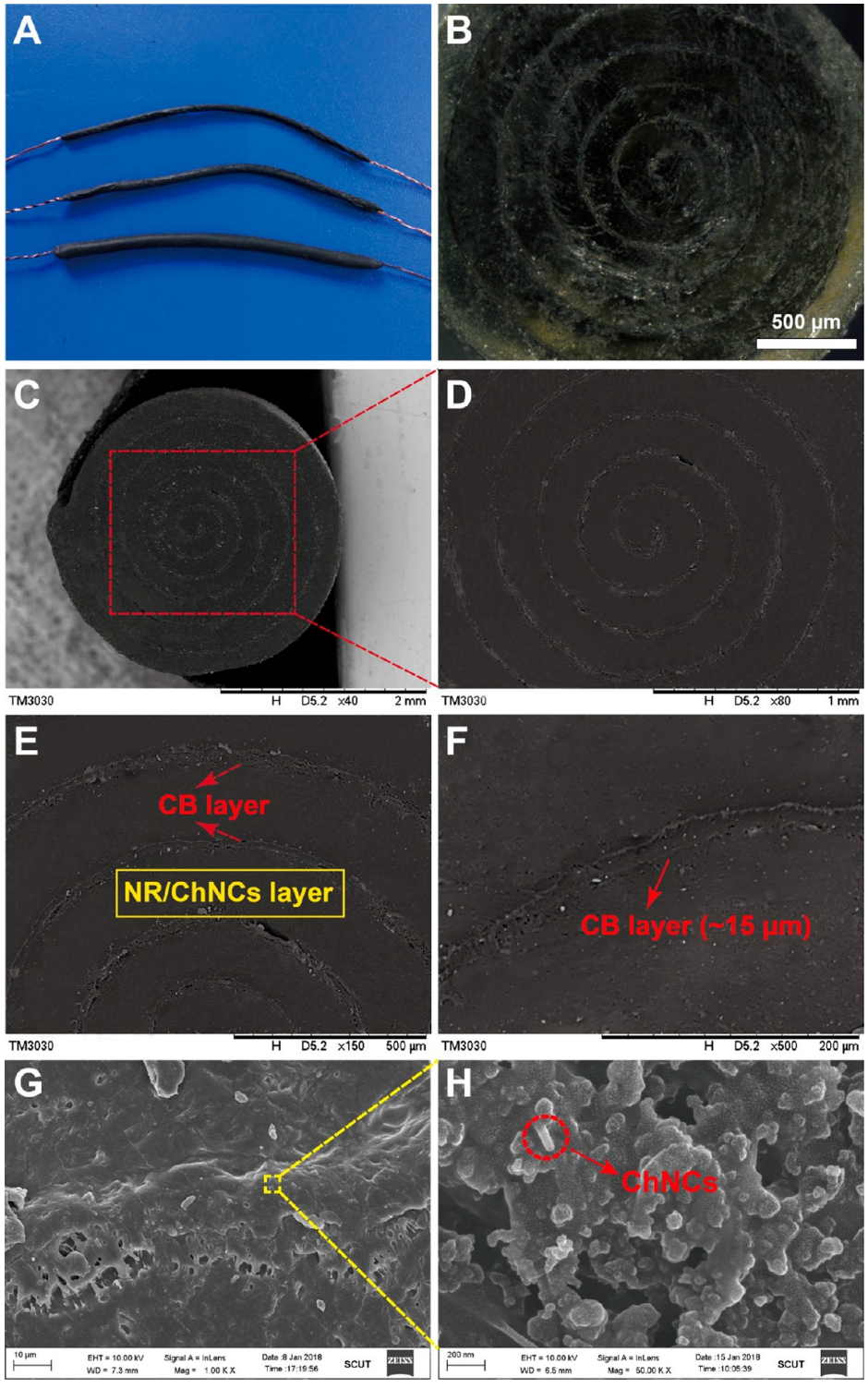

Figure 2. (A) Photograph of the as-prepared NR/ChNCs-CB composites with different diameters. (B) Optical micrograph of the spirally layered NR/ChNCs-CB composites. (C−H) SEM images of the spirally layered NR/ChNCs-CB composites with different magnification.

NR/ChNCs film were observed by an Olympus BX53 M under normal light. The cross sections of the materials were cut with scissors.

Scanning Electron Microscopy (SEM). On the cross section of the NR/ChNCs-CB composite was sprayed a gold layer of ∼20 nm thickness with a SBC-12 ion sputter coater (KYKY Technology Co.,LTD, China) before observation using a ZEISS Ultra 55 SEM. The CB layer formed on the surface of the NR/ChNCs material film by thermal spraying can be observed directly on a ZEISS Ultra 55 SEM without spraying gold.

Mechanical Property Test. Tensile properties of a round strips of the NR/ChNCs-CB composites were measured using a universal testing machine (UTM-Q422, China Chengde Jinjian Testing Instrument Co., Ltd.), and the tensile rate was 50 mm/min. The tensile rate of the material in a cycle test was also 50 mm/min.

Conductivity Measurement. The electrical conductivity of the composite sample was measured by a multimeter (Fluke 17B+, R > 2

DOI: 10.1021/acssuschemeng.8b01933
ACS Sustainable Chem. Eng. XXXX, XXX, XXX−XXX

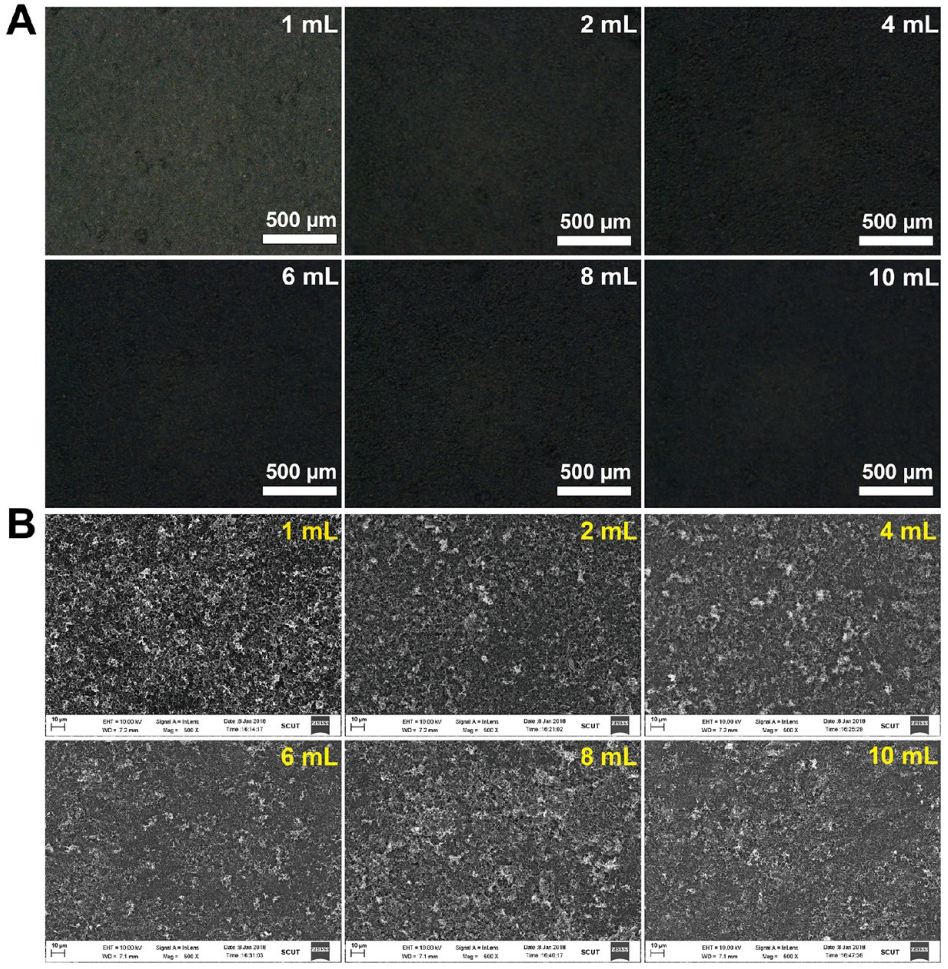

Figure 3. (A) Optical micrograph of CB layer with different amounts of CB suspension. (B) SEM images of CB layer with different amounts of CB suspension.

$\times 10^8$ Ω), and the resistance of the sample was measured using the two-point method. The calculation formula for its conductivity is

$$G = \frac{L}{RS}$$

where L is the length of the conductor, and S is the cross-sectional area of the conductor.

Sensor Application Test. The spirally layered NR/ChNCs-CB composite was applied to the wearable device, which was attached to the finger joints, hand joints, cervical vertebrae, and throat, and the resistance change signals were recorded by the TEGAM 1740 micro-ohm meter.

RESULTS AND DISCUSSION

Structure and Mechanical Properties of NR/ChNCs-CB Conductive Composites. NR/ChNCs-CB composites with spirally layered structures were prepared by a simple thermal spraying method. The specific preparation process is shown in Figure S1. After spraying a layer of NR/ChNCs film on the glass, the copper wire is fixed on the two sides of the film by a conductive adhesive. The second layer (CB layer) and the third layer (NR/ChNCs film) are covered by spraying; then, it is rolled into a round strip of conductive composite. Figure 2A shows the spirally layered NR/ChNCs-CB composite with a strip shape. The preparation process of the composite is simple, environmentally friendly, and easy to control variables. By controlling the spraying volume of the NR/ChNCs dispersion, different diameters of the striped NR/ChNCs-CB composites can be obtained. The diameters of the spirally layered composites in the picture are 1.5, 2.5, and 4 mm, respectively. However, it is hard to roll if the diameters of the spirally layered composites further decrease. Figure 2B shows an optical microphotograph of a smooth cross section of a NR/ChNCs-CB composite (CB content is 4.44%). In the composite, the CB layer and the NR/ChNCs layer of the spiral structure are spaced apart and alternated, resulting in a special alternating and spiral-stratified structure. The SEM image of the cross section is shown in Figure 2C. The slightly bright spiral lines are CB layers, and the dark gray regions are NR/ChNCs matrices, which also confirm the formation of alternately separated spirally layered structures across the entire cross section of the composite material. In Figure 2D, the central portion of the composite material is magnified by 80X, and the CB layer can be clearly identified in the SEM image which exhibits an Archimedean spiral pattern on the matrix. By further magnification, it is found that the CB layer and the NR/ChNCs layer have relatively clear boundaries, and the thicknesses of NR/ChNCs are ∼250 μm (Figure 2E), while the thickness of the CB layer is ∼15 μm (Figure 2F). Figure 2H displays a SEM image of the CB layer partially enlarged to 50,000X; the granular CB is clearly identified in this image. It is also found that the surface of the CB layer is covered with a thin rubber film, which effectively prevents the

DOI: 10.1021/acssuschemeng.8b01933
ACS Sustainable Chem. Eng. XXXX, XXX, XXX−XXX

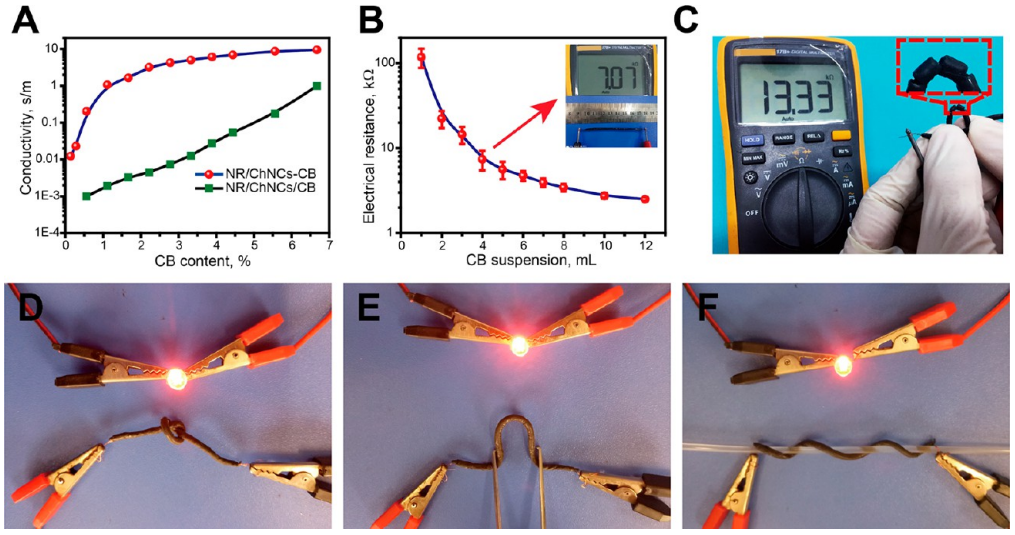

Figure 4. (A) Electrical conductivity of the spirally layered NR/ChNCs-CB composites and NR/ChNCs/CB composites. (B) Electrical resistance of the spirally layered NR/ChNCs-CB composites at different CB contents (inset showing the measuring method of resistance). (C) Photograph showing that when NR/ChNCs-CB composites are partially cut, they still have electrical conductive. Photographs showing the stable illumination of the LED light when the NR/ChNCs-CB composites were knotted (D), bent (E), and twisted (F).

CB from falling off. The CB layer firmly adheres between the interlayers of the NR/ChNCs matrix, ensuring the stability of the conductive path. The layered spiral structure can achieve good electrical conductivity by adding a small amount of CB. After careful observation, the traces of rod-shaped ChNCs can be found in the high-magnificaion image, which are embedded in the CB layer. Moreover, this new spirally layered structure is seldom reported in other literatures.[10,47]

Different volumes of CB ethanol dispersion were sprayed on the surface of the NR/ChNCs film, and then, the morphology of the CB layer was observed in the vertical direction. As shown in Figure 3A, under the optical microscope, it is observed that CB is adhered evenly to the NR/ChNCs matrix. With more CB spraying (the volume of CB ethanol dispersion is sprayed from 1 to 10 mL), the thicker the CB layer is and the worse the transmittance is. Under the SEM observation, granular CB adhered to the rubber surface can be observed clearly. As shown in Figure 3B, CB uniformly stacked on the surface of the NR/ChNCs matrix and formed conductive pathways. With the increase in the CB loading, the surface morphology becomes more flat due to the dense packing of CB particles. Compared with the conventional conductive filler in composites randomly dispersed in the matrix, this coating structure can achieve high conductivity in the case of a small amount of CB, which also simplifies the preparation process and reduces the manufacturing cost.

Figure S2 displays the SEM images showing the CB layer and CB layer covered by the NR/ChNCs thin film. The SEM image of the CB layer is shown in Figure S2A, and the CB is stacked to form a concave and convex shape. Because there is no strong interaction among CB, the structure is loose and the CB of the matrix surface will fall off easily. Figure S2B shows the morphology of the CB layer covered by a NR/ChNCs film. When the surface of the CB layer is uniformly sprayed with the NR/ChNCs dispersion, a NR/ChNCs composite forms an adhesion layer on the surface of the CB, which ensures the structural stability of the conductive path.

As one-dimensional nanomaterials, ChNCs have an excellent reinforcing ability toward polymers. ChNCs exhibit a rod-like structure with a width of ~40 nm and length between 150 and 1000 nm, which gives an aspect ratio of 3.75−25 (Figure S3A). ChNCs show an average size of 77.5 ± 8.6 nm by dynamic light scattering techniques (Figure S3B). The zeta potential of the ChNCs dispersion is +34.8 mV, which means that ChNCs have good dispersion and stability in an aqueous solution. ChNCs can be uniformly dispersed in the natural rubber matrix through the solution mixing method and effectively improve the mechanical properties of the rubber. In our previous work, it is found that when the content of ChNCs was 5%, the tensile strength of the composite material was greatly improved while a small amount of elongation at break was lost.[45] Therefore, a 5% ChNCs content of NR/ChNCs composite is chosen as the matrix of the NR/ChNCs-CB sensor material in this study, and the content of CB is 4.44%. As shown in Figure S4A, the tensile strength of the NR-CB composite is 1.12 ± 0.23 MPa, while the tensile strength of the NR/ChNCs-CB composite is 3.47 ± 0.51 MPa; that is nearly 3.1 times that of the NR-CB composite. Moreover, the elongation at break of the NR/ChNCs-CB composite is 623 ± 35%, indicating it is still a highly stretchable elastomer. CB nearly is neutral or slightly negatively charged (~10.0 mV) due to the oxygen-containing groups on their surfaces, while ChNCs are positively charged. Therefore, there are electrostatic interactions between ChNCs and CB. In addition, the hydrogen bonding interaction between ChNCs and CB may also exist. The IR peaks around 3450 cm^{-1} attributed to the stretching vibration of OH groups and phenolic hydroxyl groups on the CB surfaces have shifted to 3436 cm^{-1} in the ChNCs/CB hybrid, suggesting hydrogen bonding interactions between them (Figure S5A).[48] However, the interactions between ChNCs and CB cannot be identified from XRD results (Figure S5B). The interactions are beneficial for the increase in tensile properties of NR. Figure S4B shows the cyclical tensile test results of NR/ChNCs-CB composites. The mechanical hysteresis effect of the NR/ChNCs-CB composite is shown in the first stretch−release period, which may be attributed to the rearrangement of the rubber macromolecules during the first stretching process. After the first cycle, the

DOI: 10.1021/acssuschemeng.8b01933
ACS Sustainable Chem. Eng. XXXX, XXX, XXX−XXX

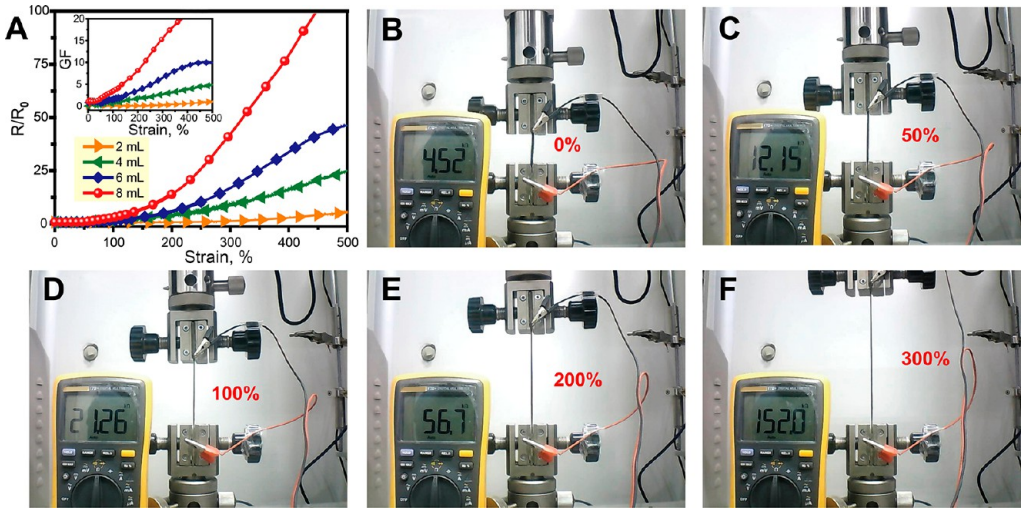

Figure 5. (A) Conductive stability of the NR/ChNCs-CB composites, variation in resistance and GF (inset) of NR/ChNCs-CB composites with different CB contents under increasing strain. (B–F) Photographs showing electrical resistance of the NR/ChNCs-CB composites increasing strain from 0% to 300%.

stretch–release cycle curves are almost overlapped, which indicates that NR/ChNCs-CB composites have good elasticity.

Conductivity of NR/ChNCs-CB Conductive Composites. Figure 4A shows the electrical conductivity of NR/ChNCs-CB composites and NR/ChNCs/CB composites with different CB contents. When CB content is 0.56%, the conductivity of NR/ChNCs-CB composite is 0.202 s/m. The conductivity of the composite increases rapidly when the spraying amount of CB ethanol dispersions increases to 4.44%, and its conductivity reaches 6.92 s/m. As the CB content continues to increase, the electrical conductivity of the composite material tends to increase slowly. When the spraying amount of the CB ethanol dispersion is 6.67%, the conductivity of the composite material is 9.51 s/m. In contrast, the electrical conductivity of the NR/ChNCs/CB ternary composites prepared by the solution mixing–casting method is far lower than the composites of the spirally layered structure at the same CB content. For example, the conductivity of the ternary composite is only 0.99 s/m when the CB content is 6.67%. When the CB content of the NR/ChNCs-CB composites prepared by solution mixing–spraying–rolling is 0.28%, the conductivity of the sample begins to increase rapidly, while the percolation threshold of NR/ChNCs/CB composites is 2.22%. This can be explained by CB being embedded in the rubber matrix by the solution mixing method, so the conductivity of the composites is relatively low. CB in the spirally structured composites can form a continuous conductive path at relatively low content, which increase the conductivities. Figure 4B shows the relationship between the resistance of the composites and the volume of the CB ethanol dispersions. The resistance of the NR/ChNCs-CB composite can be effectively tailored by controlling the volume of the CB ethanol dispersion. With the increase in sprayed CB ethanol dispersion on NR/ChNCs film, the resistance of the CB layer decreases correspondingly, revealing the gradual construction of a CB conductive channel. The inset in Figure 4B is the method to measure resistance of the composite with a multimeter. In Figure 4C, the NR/ChNCs-CB composite is partially cut at three sites, but the material still has conductivity, indicating that the composite has good conductive stability. Further validation such as knots, bends, and twists do not change the lighting of the LED lamp (Figure 4D, E), illustrating that the NR/ChNCs-CB composite is a conductor with excellent flexibility and stability. The spirally layered NR/ChNCs-CB composite is conductive in the inner part and insulated at the outer surface, so the structure and shape are similar to the wires. But commercial wires composed with a copper line as the core and rubber as the outer skin cannot be stretched since they are easily destroyed. In contrast, the prepared NR/ChNCs-CB composite is a stretchable conductor.

Performance of NR/ChNCs-CB Strain Sensor. Figure 5A illustrates the curve of resistance variation (R/R_0) and gauge factor (GF) of a NR/ChNCs-CB composite with strain. It can be found that by increasing the thickness of the CB layer the resistance changes with strain become greater especially at large strains (>150%). This is because the surface of the CB layer covers the NR/ChNCs layer and makes the structure of the CB layer stable while the structure is fixed. When the material bears strain, the CB in the composites does not slip. This is also demonstrated by the GF-strain curve of NR/ChNCs-CB composites. The NR/ChNCs-CB composite of a spirally layered structure prepared by spraying 8 mL of CB ethanol suspension (corresponding CB content of 4.44%) shows good conductivity and strain sensitivity, which can be used as a flexible sensor. Figure 5B–F records the change of resistance of this NR/ChNCs-CB composite with different strain. When the strains are 50%, 100%, 200%, and 300%, the R/R_0 values of the composites are 2.69, 4.70, 12.54, and 33.63, respectively. The change of resistance of the composites is consistent with that of the NR/ChNCs-CB composite material (8 mL) in Figure 5A.

NR/ChNCs-CB composites with a CB content of 4.44% were selected as strain sensors in the latter part. Figure 6A shows the variation curve of the relative resistance R/R_0 of the strain sensor during the first stretch–release cycle at a tensile strain of 50%. It is found that the R/R_0 of the strain sensor fails to return to 1 after the first stretching cycle, which is attributed to the mechanical hysteresis effect of the elastomer. The rearrangement of the rubber macromolecular chain leads to delayed deformation during the first stretching process, which is in accordance with the results of the cyclic tensile test of the

DOI: 10.1021/acssuschemeng.8b01933
ACS Sustainable Chem. Eng. XXXX, XXX, XXX–XXX

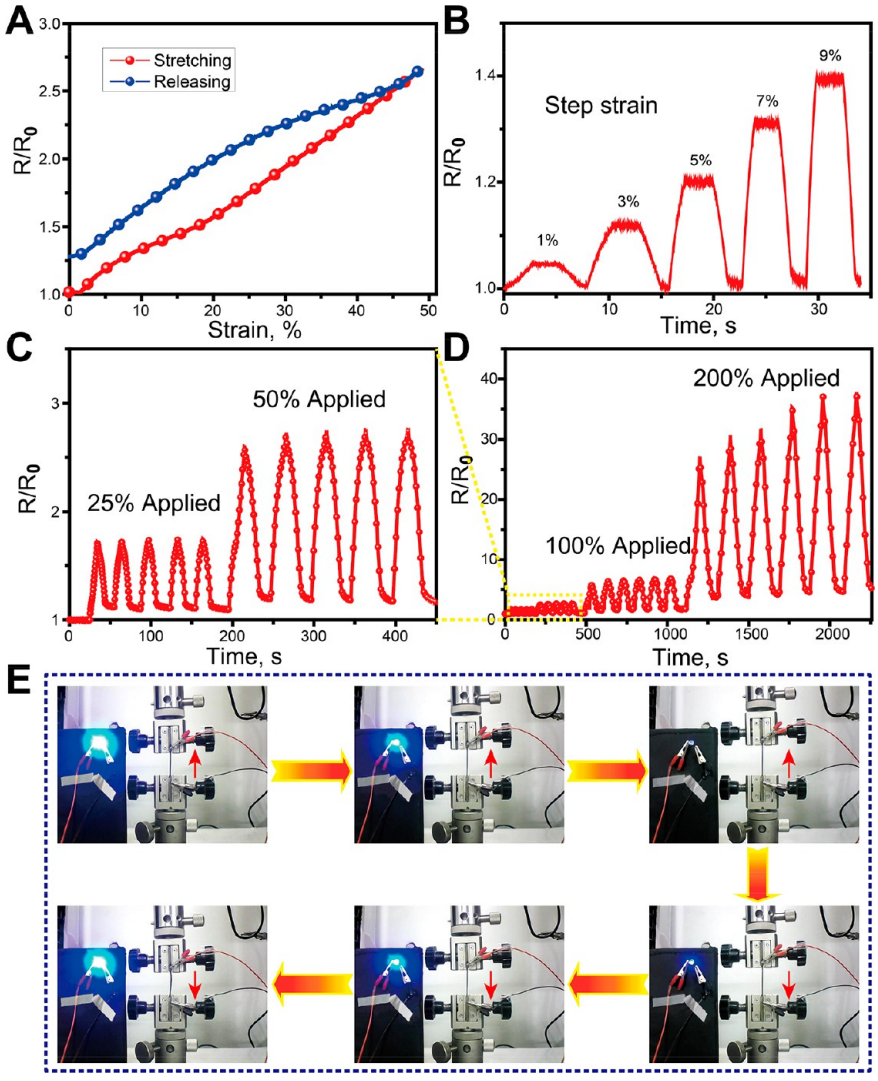

Figure 6. (A) Changes in relative resistance under a 50% strain stretching−releasing cycle. (B) Relative resistance variation under gradually increasing step strain from 1% to 9% strain. (D) Dynamic stretch−release cycle response of the sensor for various strains 25%−200%. (C) Stretch−release cycles for 25% and 50%. (E) Photographs showing a lighted LED light changing with the strain of NR/ChNCs-CB composites under a 50% strain stretch−release cycle.

composite. The resistance of strain sensor changes with the change of deformation, and the resistance is higher at the releasing process than that at the stretching process due to the partially destroyed conductive network upon stretching. Figure 6B displays the change in relative resistance R/R_0 at increasing step strains. In the small strain range, strain sensors have higher sensitivity. According to the GF formula (GF = $(\Delta R/R_0)/(\Delta L/L)$), the strain sensor of GF is calculated (GF ≈ 5) within a small deformation range. The mechanism of the high sensitivity of the spirally structured rubber composites is related to composite formulation and structure. When the CB content reaches a certain amount, the conductive paths are formed in the composites. In addition, CB is tightly stacked on the NR/ChNCs matrix layer with a high adhesion force with the rubber matrix (Figure 3). The NR/ChNCs composite has a good elasticity, so the CB conductive network can sensitively response the external strain. The conductivity decreases when the composites are stretched, while the conductivity increases when the deformation of the composites is recovered. The spirally structured rubber composites with 4.44% CB content show relatively rapid variation in resistance under strain, making them suitable to serve as stretchable sensors that require desired sensitivity to deformations. When the CB content exceeds 4.44%, the structure of the material is unstable because the CB layer is too thick. Compared with the other reported strain sensors (see Table S1), the NR/ChNCs-CB strain sensor has both high tensile properties and higher GF. For instance, the Ag nanowires−PDMS nanocomposite-based strain sensors show piezoresistivity with tunable GF in the ranges from 2 to 14 but only have stretchability of 70%. Therefore, the NR/ChNCs-CB composite is an excellent candidate for the wearable equipment.

The strain sensitivity of the sensor at large strain was then studied. Figure 6C and D shows the changes in the relative resistance R/R_0 of the strain sensors in five tensile−release cycles of 25%, 50%, 100%, and 200%. It is clearly seen from the diagram that the relative resistance R/R_0 of the sensor is slightly higher than that of the original R/R_0 in the first stretch−release cycle of each large deformation, and the composite shows excellent elasticity and resilience in the subsequent stretch−release cycle. Therefore, the prepared strain sensor has excellent stability and elasticity under

DOI: 10.1021/acssuschemeng.8b01933
ACS Sustainable Chem. Eng. XXXX, XXX, XXX−XXX

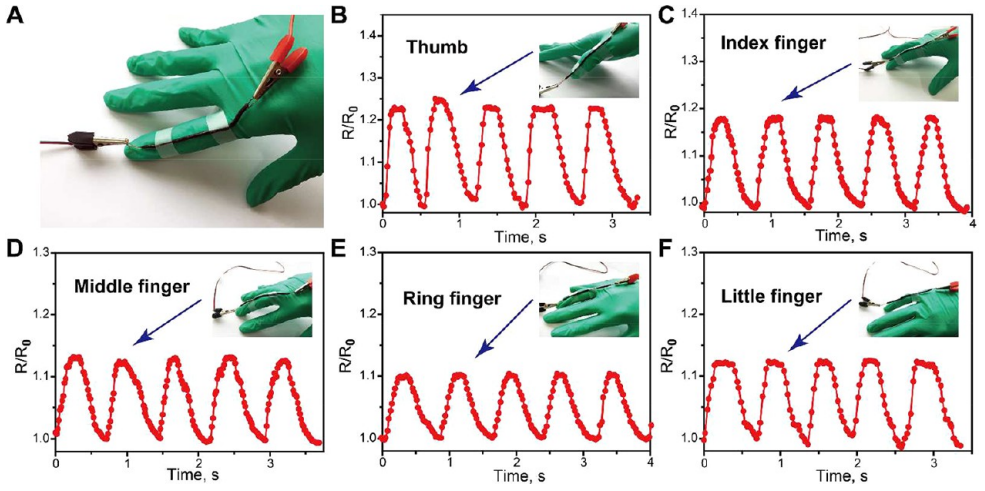

Figure 7. (A) Photographs showing the strain sensor attached to a latex glove for recording the movements of the index finger. (B–F) Results of motion detection of the finger.

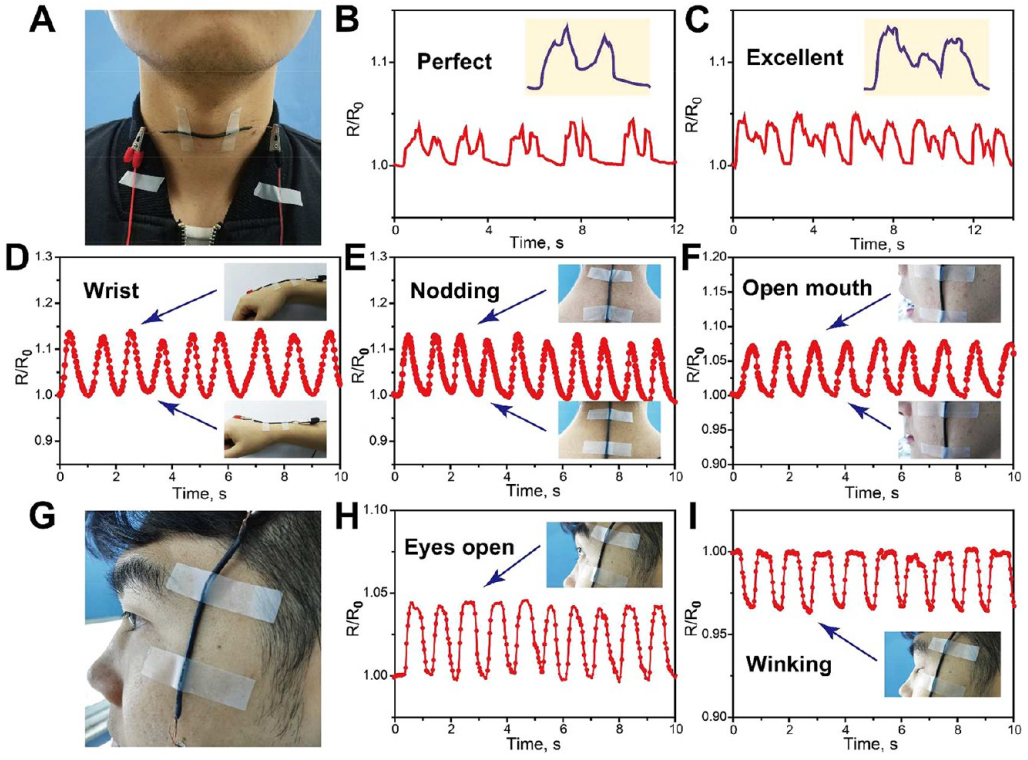

Figure 8. Photograph showing the strain sensor attached to the throat (A) and recorded current signals when the tester pronounced different words (B, C) and conducted diverse physiological activities (D–F). Picture of a sensor attached to a cheek (G) and recorded current patterns when the tester conducted different eye movements (H, I).

maximum strain of 200%. Figure 6E recorded the change in lamp brightness with strain during the stretch–release cycle of the strain sensor. When the sensor is stretched, the resistance becomes larger, and the light brightness becomes darker. In the process of release, the resistance of the sensor becomes smaller, and the light begins to brighten again. In addition, the first SI video shows the changes of the small lamp in the 50% and 100% stretch–release cycle of the strain sensor, and the second SI video shows the change of the small lamp in the 50% cycle stretching of the strain sensor for several times. All these results suggest that the conductivity of the sensor can be changed rapidly with the strain, and the NR/ChNCs-CB composite can be designed as a wearable device.

Application of NR/ChNCs-CB Strain Sensor in Wearable Devices. Because of the high sensitivity and low detection limit of the NR/ChNCs-CB sensor, it can be used in wearable devices. In Figure 7, the strain sensor is attached to a latex glove worn by a volunteer to detect the flexural movement of finger joints. The measured index finger is naturally held upright as an initial state of finger bending motion, as shown in Figure 7A. When the finger is bent, the strain sensor has a certain deformation, and the resistance of the sensor increases with the strain. After the finger is relaxed,

DOI: 10.1021/acssuschemeng.8b01933
ACS Sustainable Chem. Eng. XXXX, XXX, XXX–XXX

the sensor is restored to the initial state, and its resistance goes back to the initial value. During this test, each finger of the hand is tested and repeated for five cycles (Figure 7B−F); it also can be seen that the sensor has a highly stability and recovery performance.

To further verify whether NR/ChNCs-CB strain sensors can detect tiny human activities, the sensor is used to monitor small-scale physiological activities of the human body such as pronunciation, bending of the wrist, nodding, opening the mouth, and eyes opening and winking. Figure 8A shows the strain sensor attached to near the throat of the tester during detecting pronunciation. When the tester speaks different words (such as perfect and excellent), the sensor produces characteristic electrical signals associated with the different words (Figure 8B, C). This is because each word causes a specific form of muscle movement in the throat, giving a distinct electrical signal. The difference in these electrical signals shows the good potential of the strain sensor as a speech recognition device. In addition, volunteers can also paste the strain sensor on other parts for testing, such as hand joints, neck, and mouth corner, and the related characteristic signals are also recorded, as shown in Figure 8D−F. It shows that the strain sensor has good reproducibility and reliability. The strain sensor was also attached to the cheek near the eye to detect volunteer eye movement as shown in Figure 8G. When the eyes are open (Figure 8H) or closed (Figure 8I), the difference and repeatable electrical signal changes are caused. This means the strain sensor can monitor tiny facial expression. Therefore, based on monitoring the capacity of small-scale physiological activity, NR/ChNCs-CB strain sensors can be expected to be used in the manufacture of diversified healthcare equipment and the establishment of a convenient control system on the patient's body.

CONCLUSIONS

In this study, a new type of highly stretchable, high-strength, and cost-competitive conductive composite was developed through a simple solution mixing−spraying−rolling method. The NR/ChNCs matrix is tightly bonded on the CB layer to form a stable layered structure, and then, a spirally structured conductive composite is obtained by rolling the sheets. This structure is conductive with a small amount of CB. When the CB content is 4.44%, the conductivity can reach 6.92 s/m. The conductive properties of composites are effectively tailored by controlling the thickness of the CB layer. The composite shows a GF of 5, which has the characteristics of good conductivity, good stretchability, structural stability, and variable strain sensitivity. These advantages enable composites to be prepared as multifunctional sensors for monitoring small and large human activities, as well as devices for wearable electronics. They can effectively monitor the small-scale physiological activities of the human body such as finger movements, pronunciation, bending of the wrist, nodding, opening the mouth, and eyes opening and winking. This study has prepared highly stretchable and multifunctional electronic products based on inexpensive raw materials in a simple manner, which opens new opportunities for the manufacture and practical application of stretchable electronic devices.

ASSOCIATED CONTENT

Supporting Information

The Supporting Information is available free of charge on the ACS Publications website at DOI: 10.1021/acssuschemeng.8b01933.

Preparation process of the spirally layered NR/ChNCs-CB composites; 30,000X magnification of SEM image of CB layer and after coating NR/ChNCs suspension; TEM image, zeta potential, and size distribution of ChNCs in aqueous dispersion; results of tensile and cyclic tensile tests of the composite; FTIR spectra and XRD patterns of CB, ChNCs, and ChNCs/CB hybrids; summary of performance of some recently reported strain sensors. (PDF)

Video showing the changes of the small lamp in the 50% and 100% stretch−release cycle of the strain sensor. (AVI)

Video showing the change of the small lamp in the 50% cycle stretching of the strain sensor several times. (AVI)

AUTHOR INFORMATION

Corresponding Author

*E-mail: liumx@jnu.edu.cn. Tel/Fax: +86-20-8522 3271.

ORCID

Mingxian Liu: 0000-0002-5466-3024

Author Contributions

The manuscript was written through the contributions of all authors. All authors have given approval to the final version of the manuscript.

Notes

The authors declare no competing financial interest.

ACKNOWLEDGMENTS

This work was financially supported by the National Natural Science Foundation of China (51473069 and 51502113), Guangdong Natural Science Funds for Distinguished Young Scholar (S2013050014606), Guangdong Special support program (2014TQ01C127), Science and Technology PlanningProject of Guangdong Province (2014A020217006), and Pearl River S&T Nova Program of Guangzhou (201610010026).

REFERENCES

(1) Huang, Y.; Kershaw, S. V.; Wang, Z.; Pei, Z.; Liu, J.; Huang, Y.; Li, H.; Zhu, M.; Rogach, A. L.; Zhi, C. Highly Integrated Supercapacitor-Sensor Systems via Material and Geometry Design. *Small* **2016**, *12* (25), 3393−3399.

(2) Sekitani, T.; Nakajima, H.; Maeda, H.; Fukushima, T.; Aida, T.; Hata, K.; Someya, T. Stretchable Active-Matrix Organic Light-Emitting Diode Display Using Printable Elastic Conductors. *Nat. Mater.* **2009**, *8* (6), 494−499.

(3) Yao, S.; Zhu, Y. Wearable Multifunctional Sensors Using Printed Stretchable Conductors Made of Silver Nanowires. *Nanoscale* **2014**, *6* (4), 2345−2352.

(4) Wang, Z.; Huang, Y.; Sun, J.; Huang, Y.; Hu, H.; Jiang, R.; Gai, W.; Li, G.; Zhi, C. Polyurethane/Cotton/Carbon Nanotubes Core-Spun Yarn as High Reliability Stretchable Strain Sensor for Human Motion Detection. *ACS Appl. Mater. Interfaces* **2016**, *8* (37), 24837−24843.

(5) Chen, S.; Wei, Y.; Yuan, X.; Lin, Y.; Liu, L. A highly Stretchable Strain Sensor Based on a Graphene/Silver Nanoparticle Synergic Conductive Network and a Sandwich Structure. *J. Mater. Chem. C* **2016**, *4* (19), 4304−4311.

DOI: 10.1021/acssuschemeng.8b01933
ACS Sustainable Chem. Eng. XXXX, XXX, XXX−XXX

(6) Jang, H.; Park, Y. J.; Chen, X.; Das, T.; Kim, M. S.; Ahn, J. H. Graphene-Based Flexible and Stretchable electronics. *Adv. Mater.* **2016**, *28* (22), 4184−4202.
(7) Cao, J.; Lu, C.; Zhuang, J.; Liu, M.; Zhang, X.; Yu, Y.; Tao, Q. Multiple Hydrogen Bonding Enables the Self-Healing of Sensors for Human-Machine Interaction. *Angew. Chem., Int. Ed.* **2017**, *56*, 8795−8800.
(8) Liu, X.; Su, G.; Guo, Q.; Lu, C.; Zhou, T.; Zhou, C.; Zhang, X. Hierarchically Structured Self-Healing Sensors with Tunable Positive/Negative Piezoresistivity. *Adv. Funct. Mater.* **2018**, *28*, 1706658.
(9) Guo, Q.; Luo, Y.; Liu, J.; Zhang, X.; Lu, C. A Well-organized Graphene Nanostructure for Versatile Strain-sensing Application Constructed by a Covalently Bonded Graphene/Rubber Interface. *J. Mater. Chem. C* **2018**, *6*, 2139−2147.
(10) Wu, X.; Han, Y.; Zhang, X.; Lu, C. Spirally Structured Conductive Composites for Highly Stretchable, Robust Conductors and Sensors. *ACS Appl. Mater. Interfaces* **2017**, *9* (27), 23007−23016.
(11) Liu, Y.; Zheng, H.; Liu, M. High Performance Strain Sensors Based on Chitosan/Carbon Black Composite Sponges. *Mater. Des.* **2018**, *141*, 276−285.
(12) Yi, F.; Lin, L.; Niu, S.; Yang, P. K.; Wang, Z.; Chen, J.; Zhou, Y.; Zi, Y.; Wang, J.; Liao, Q.; et al. Stretchable-Rubber-Based Triboelectric Nanogenerator and Its Application as Self-powered Body Motion Sensors. *Adv. Funct. Mater.* **2015**, *25* (24), 3688−3696.
(13) Lin, Y.; Liu, S.; Chen, S.; Wei, Y.; Dong, X.; Liu, L. A Highly Stretchable and Sensitive Strain Sensor Based on Graphene−Elastomer Composites with a Novel Double-Interconnected Network. *J. Mater. Chem. C* **2016**, *4* (26), 6345−6352.
(14) Yang, P. K.; Lin, L.; Yi, F.; Li, X.; Pradel, K. C.; Zi, Y.; Wu, C. I.; He, H., Jr; Zhang, Y.; Wang, Z. L. A Flexible, Stretchable and Shape-Adaptive Approach for Versatile Energy Conversion and Self-Powered Biomedical Monitoring. *Adv. Mater.* **2015**, *27* (25), 3817−3824.
(15) Boland, C. S.; Khan, U.; Ryan, G.; Barwich, S.; Charifou, R.; Harvey, A.; Backes, C.; Li, Z.; Ferreira, M. S.; Möbius, M. E.; et al. Sensitive Electromechanical Sensors Using Viscoelastic Graphene-Polymer Nanocomposites. *Science* **2016**, *354* (6317), 1257−1260.
(16) Ren, J.; Wang, C.; Zhang, X.; Carey, T.; Chen, K.; Yin, Y.; Torrisi, F. Environmentally-Friendly Conductive Cotton Fabric as Flexible Strain Sensor Based on Hot Press Reduced Graphene Oxide. *Carbon* **2017**, *111*, 622−630.
(17) Shi, G.; Zhao, Z.; Pai, J. H.; Lee, I.; Zhang, L.; Stevenson, C.; Ishara, K.; Zhang, R.; Zhu, H.; Ma, J. Highly Sensitive, Wearable, Durable Strain Sensors and Stretchable Conductors Using Graphene/Silicon Rubber Composites. *Adv. Funct. Mater.* **2016**, *26* (42), 7614−7625.
(18) Cai, G.; Wang, J.; Qian, K.; Chen, J.; Li, S.; Lee, P. S. Extremely Stretchable Strain Sensors Based on Conductive Self-Healing Dynamic Cross-Links Hydrogels for Human-Motion Detection. *Adv. Sci.* **2017**, *4*, 1600190.
(19) Pang, C.; Lee, G.-Y.; Kim, T.-i.; Kim, S. M.; Kim, H. N.; Ahn, S. H.; Suh, K. Y. A Flexible and Highly Sensitive Strain-Gauge Sensor Using Reversible Interlocking of Nanofibres. *Nat. Mater.* **2012**, *11* (9), 795−801.
(20) Gong, S.; Schwalb, W.; Wang, Y.; Chen, Y.; Tang, Y.; Si, J.; Shirinzadeh, B.; Cheng, W. A Wearable and Highly Sensitive Pressure Sensor with Ultrathin Gold Nanowires. *Nat. Commun.* **2014**, *5*, 3132.
(21) Tian, H.; Shu, Y.; Wang, X. F.; Mohammad, M. A.; Bie, Z.; Xie, Q. Y.; Li, C.; Mi, W. T.; Yang, Y.; Ren, T. L. A Graphene-Based Resistive Pressure Sensor with Record-High Sensitivity in a Wide Pressure Range. *Sci. Rep.* **2015**, *5*, 8603.
(22) Tian, H.; Shu, Y.; Cui, Y. L.; Mi, W. T.; Yang, Y.; Xie, D.; Ren, T. L. Scalable Fabrication of High-performance and Flexible Graphene Strain Sensors. *Nanoscale* **2014**, *6* (2), 699−705.
(23) Yu, Y.; Luo, S.; Sun, L.; Wu, Y.; Jiang, K.; Li, Q.; Wang, J.; Fan, S. Ultra-stretchable Conductors Based on Buckled Super-aligned Carbon Nanotube Films. *Nanoscale* **2015**, *7* (22), 10178−10185.
(24) Cheng, Y.; Wang, R.; Sun, J.; Gao, L. Highly Conductive and Ultrastretchable Electric Circuits from Covered Yarns and Silver Nanowires. *ACS Nano* **2015**, *9* (4), 3887−3895.
(25) Qi, D.; Liu, Z.; Liu, Y.; Leow, W. R.; Zhu, B.; Yang, H.; Yu, J.; Wang, W.; Wang, H.; Yin, S.; et al. Suspended Wavy Graphene Microribbons for Highly Stretchable Microsupercapacitors. *Adv. Mater.* **2015**, *27* (37), 5559−5566.
(26) Choi, D. Y.; Kim, M. H.; Oh, Y. S.; Jung, S. H.; Jung, J. H.; Sung, H. J.; Lee, H. W.; Lee, H. M. Highly Stretchable, Hysteresis-free Ionic Liquid-based Strain Sensor for Precise Human Motion Monitoring. *ACS Appl. Mater. Interfaces* **2017**, *9* (2), 1770−1780.
(27) Liang, J.; Li, L.; Tong, K.; Ren, Z.; Hu, W.; Niu, X.; Chen, Y.; Pei, Q. Silver Nanowire Percolation Network Soldered with Graphene Oxide at Room Temperature and Its Application for Fully Stretchable Polymer Light-emitting Diodes. *ACS Nano* **2014**, *8* (2), 1590−1600.
(28) Wu, X.; Han, Y.; Zhang, X.; Zhou, Z.; Lu, C. Large-Area Compliant, Low-Cost, and Versatile Pressure-Sensing Platform Based on Microcrack-Designed Carbon Black@Polyurethane Sponge for Human-Machine Interfacing. *Adv. Funct. Mater.* **2016**, *26* (34), 6246−6256.
(29) Zhu, C.; Han, T. Y.-J.; Duoss, E. B.; Golobic, A. M.; Kuntz, J. D.; Spadaccini, C. M.; Worsley, M. A. Highly Compressible 3D Periodic Graphene Aerogel Microlattices. *Nat. Commun.* **2015**, *6*, 6962.
(30) Xu, F.; Wang, X.; Zhu, Y.; Zhu, Y. Wavy Ribbons of Carbon Nanotubes for Stretchable Conductors. *Adv. Funct. Mater.* **2012**, *22* (6), 1279−1283.
(31) Liang, J.; Zhang, G.; Chen, X.; Wang, W. In *Strain Gauges Based Force Sensor for Precision Assembly of Helix Slow-Wave Structure, Manipulation, Automation and Robotics at Small Scales (MARSS)*; International Conference on IEEE: 2016; pp 1−6. DOI: 10.1109/MARSS.2016.7561738.
(32) Won, Y.; Kim, A.; Yang, W.; Jeong, S.; Moon, J. A Highly Stretchable, Helical Copper Nanowire Conductor Exhibiting a Stretchability of 700%. *NPG Asia Mater.* **2014**, *6* (9), e132.
(33) Guo, H.; Chen, J.; Leng, Q.; Xi, Y.; Wang, M.; He, X.; Hu, C. Spiral-interdigital-electrode-based Multifunctional Device: Dual-functional Triboelectric Generator and Dual-functional Self-powered Sensor. *Nano Energy* **2015**, *12*, 626−635.
(34) Jing, W.; Zhou, F.; Gao, W.; Jiang, Z.; Ren, W.; Shi, J.; Cheng, Y.; Gao, K. Regulating the Hydrothermal Synthesis of ZnO Nanorods to Optimize the Performance of Spirally Hierarchical Structure-based Glucose Sensors. *RSC Adv.* **2015**, *5* (105), 85988−85995.
(35) Lee, P.; Lee, J.; Lee, H.; Yeo, J.; Hong, S.; Nam, K. H.; Lee, D.; Lee, S. S.; Ko, S. H. Highly Stretchable and Highly Conductive Metal Electrode by Very Long Metal Nanowire Percolation Network. *Adv. Mater.* **2012**, *24* (25), 3326−3332.
(36) Yan, C.; Wang, J.; Kang, W.; Cui, M.; Wang, X.; Foo, C. Y.; Chee, K. J.; Lee, P. S. Highly Stretchable Piezoresistive Graphene−nanocellulose Nanopaper for Strain Sensors. *Adv. Mater.* **2014**, *26* (13), 2022−2027.
(37) Khan, U.; Kim, T. H.; Ryu, H.; Seung, W.; Kim, S. W. Graphene Tribotronics for Electronic Skin and Touch Screen Applications. *Adv. Mater.* **2017**, *29* (1), 1603544.
(38) Amjadi, M.; Yoon, Y. J.; Park, I. Ultra-stretchable and Skin-mountable Strain Sensors Using Carbon Nanotubes−Ecoflex Nanocomposites. *Nanotechnology* **2015**, *26* (37), 375501.
(39) Roh, E.; Hwang, B.-U.; Kim, D.; Kim, B.-Y.; Lee, N.-E. Stretchable, Transparent, Ultrasensitive, and Patchable Strain Sensor for Human−machine Interfaces Comprising a Nanohybrid of Carbon Nanotubes and Conductive Elastomers. *ACS Nano* **2015**, *9* (6), 6252−6261.
(40) He, Z.; Liu, Q.; Hou, H.; Gao, F.; Tang, B.; Yang, W. Tailored Electrospinning of WO3 Nanobelts as Efficient Ultraviolet Photodetectors with Photo-dark Current Ratios up to 1000. *ACS Appl. Mater. Interfaces* **2015**, *7* (20), 10878−10885.
(41) Muth, J. T.; Vogt, D. M.; Truby, R. L.; Mengüç, Y.; Kolesky, D. B.; Wood, R. J.; Lewis, J. A. Embedded 3D Printing of Strain Sensors

DOI: 10.1021/acssuschemeng.8b01933
ACS Sustainable Chem. Eng. XXXX, XXX, XXX−XXX

within Highly Stretchable Elastomers. *Adv. Mater.* **2014**, *26* (36), 6307−6312.
(42) Zeng, J.-B.; He, Y.-S.; Li, S.-L.; Wang, Y.-Z. Chitin Whiskers: An Overview. *Biomacromolecules* **2012**, *13* (1), 1−11.
(43) Gopalan Nair, K.; Dufresne, A. Crab Shell Chitin Whisker Reinforced Natural Rubber Nanocomposites. 2. Mechanical Behavior. *Biomacromolecules* **2003**, *4* (3), 666−674.
(44) Liu, M.; Huang, J.; Luo, B.; Zhou, C. Tough and Highly Stretchable Polyacrylamide Nanocomposite Hydrogels with Chitin Nanocrystals. *Int. J. Biol. Macromol.* **2015**, *78*, 23−31.
(45) Liu, Y.; Liu, M.; Yang, S.; Luo, B.; Zhou, C. Liquid Crystalline Behaviors of Chitin Nanocrystals and their Reinforcing Effect on Natural Rubber. *ACS Sustainable Chem. Eng.* **2018**, *6*, 325−336.
(46) Gopalan Nair, N. K.; Dufresne, A. Crab Shell Chitin Whisker Reinforced Natural Rubber Nanocomposites. 1. Processing and Swelling Behavior. *Biomacromolecules* **2003**, *4* (3), 657−665.
(47) Liu, P.; Jin, Z.; Katsukis, G.; Drahushuk, L. W.; Shimizu, S.; Shih, C.-J.; Wetzel, E. D.; Taggart-Scarff, J. K.; Qing, B.; Van Vliet, K. J.; et al. Layered and Scrolled Nanocomposites with Aligned Semi-Infinite Graphene Inclusions at The Platelet Limit. *Science* **2016**, *353* (6297), 364−367.
(48) Xiong, R.; Hu, K.; Grant, A. M.; Ma, R.; Xu, W.; Lu, C.; Zhang, X.; Tsukruk, V. V. Ultrarobust Transparent Cellulose Nanocrystal-Graphene Membranes with High Electrical Conductivity. *Adv. Mater.* **2016**, *28*, 1501−1509.

DOI: 10.1021/acssuschemeng.8b01933
ACS Sustainable Chem. Eng. XXXX, XXX, XXX−XXX